Optimal Configuration of Multitype Energy Storage for Integrated Energy Systems Considering System Reserve Value

Xun Dou, *Senior Member*, *IEEE*, *Member*, *CSEE*, Jun Wang, *Member*, *IEEE*, Zhenyuan Zhang, *Member*, *IEEE*, and Min Gao, *Member*, *IEEE*

***Abstract*—An integrated energy system (IES) contributes to improving energy efficiency and promoting sustainable energy development. For different dynamic characteristics of the system, such as demand/response schemes and complex coupling characteristics among energy sources, siting and sizing of multitype energy storage (MES) are very important for the economic operation of the IES. Considering the effect of the diversity of the IES on system reserve based on electricity, gas and heat systems in different scenarios, a two-stage MES optimal configuration model, considering the system reserve value, is proposed. In the first stage, to determine the location and charging/discharging strategies, a location choice model that minimizes the operating cost, considering the system reserve value, is proposed. In the second stage, a capacity choice model, to minimize the investment and maintenance cost of the MES, is proposed. Finally, an example is provided to verify the effectiveness of the MES configuration method in this paper in handling operational diversity and ensuring system reserve. Compared with the configuration method that disregards the system reserve value, the results show that the MES configuration method proposed in this paper can reduce the annual investment cost and operating cost and improve the system reserve value.**

***Index Terms*—Integrated energy system, multitype energy storage, optimal configuration, renewable source, system reserve value.**

NOMENCLATURE

A. Acronyms

AC	Absorption chiller.
CHP	Combined heat and power.
CCHP	Combined cooling, heating, and power.
DHS	District heating system.
EC	Electric chiller.
EES	Electrical energy storage.
EPS	Electric power distribution system.
GES	Gas energy storage.
HE	Heat exchanger.
HES	Heat energy storage.
HR	Heat recovery unit.
IES	Integrated energy system.
MES	Multitype energy storage.
NGS	Natural gas distribution system.
P2G	Power-to-gas.
T	Power transformer.

B. Sets and Indices

G	Index of the generator.
i, j, k	Index of the bus of one line in the system.
n	Index of the gas well.
s	Index of each type of energy.
$S_i^{\mathrm{pipe}+}, S_i^{\mathrm{pipe}-}$	Index of pipes connected to node i and starting and ending from node i.
t	Index of the sub-hourly time interval.

C. Constants

a_s, b_s, c_s, d_s, e_s	Cycle life factor of the s^{th} MES.
C	Specific heat capacity of the hot water.
$C_{s,t}$	Energy market price of the s^{th} energy at time t.
C_{ew}	Cost coefficient of abandoned wind.
$C_{s,\mathrm{e}}$	Cost of the unit capacity of the s^{th} MES.
$C_{s,\mathrm{m}}$	Maintenance cost per year of the s^{th} MES charging and discharging power unit.
$C_{s,\mathrm{p}}$	Unit cost of the charge and discharge of the s^{th} MES.
$C_{\mathrm{e},t}$, $C_{\mathrm{h},t}$, $C_{\mathrm{g},t}$	Prices of electricity, heat, and gas at time t.
$C_{\mathrm{ML,G}}$, $C_{\mathrm{ML,E}}$	The gas and electricity prices in the medium-long-term market.
$C_{\mathrm{SM,G,t}}$, $C_{\mathrm{SM,E,t}}$	The gas and electricity prices in the spot market.
C_{ij}	Constant related to the efficiency, temperature, length, inner diameter, and compression factor of pipe ij.

Manuscript received July 1, 2020; revised March 30, 2021; accepted July 24, 2021. Date of online publication May 6, 2022; date of current version June 17, 2023. This work was supported in part by the National Key R&D Program of China (No. 2018YFB0905000) and the Science and Technology Project of the State Grid Corporation of China (No. SGTJDK00DWJS1800232).

X. Dou (corresponding author, email: dxnjut@njtech.edu.cn; ORCID: https://orcid.org/0000-0002-2914-9736) is with the College of Electrical Engineering and Control Science, Nanjing Tech University, Nanjing 211816, China.

J. Wang is with the Research Institute of NARI Technology Co., Ltd., Nanjing 211106, China.

Z. Y. Zhang is with the School of Mechanical and Electrical Engineering, University of Electronic Science and Technology of China, Chengdu 611731, China.

M. Gao is with Falcon Computing Solutions, 10880 Wilshire Blvd Suite 1132, Los Angeles, CA 90024, USA.

DOI: 10.17775/CSEEJPES.2020.03130

d_{r}	Discount rate.
$D_{s,t}$	Reserve market price of the s^{th} energy at time t.
$\overline{E}_{\mathrm{EES}}, \underline{E}_{\mathrm{EES}}$	Upper and lower limits of the EES capacity.
$\overline{E}_{\mathrm{GES}}, \underline{E}_{\mathrm{GES}}$	Upper and lower limits of the GES capacity.
G_{ij}, B_{ij}	Conductance and susceptance between nodes i and j.
$\overline{G}_{s,t}$	System output upper limit of the s^{th} energy.
$\overline{H}_{\mathrm{HES}}, \underline{H}_{\mathrm{HES}}$	Upper and lower limits of the HES capacity.
i_{r}	Rate of inflation.
L_{e}	Load consumption of electricity.
L_{g}	Load consumption of gas.
L_{h}	Load consumption of heat.
L_{c}	Load consumption of cooling.
M_{ij}	Constant related to the length, radius, temperature, gas density, compression factor of pipe ij.
$\overline{N}_{\mathrm{EES}}, \overline{N}_{\mathrm{GES}}, \overline{N}_{\mathrm{HES}}$	Max number of EES, GES and HES.
$P_{i,t}^{\mathrm{EL}}$	Load active power of node i at time t.
$\overline{P}_{ij}$	Active power transmission upper limit of the line between nodes i and j at time t.
$\overline{P}_{\mathrm{g}}, \underline{P}_{\mathrm{g}}$	Upper and lower limits of the active power output of the g^{th} generator.
$\overline{p}_i, \underline{p}_i$	Upper and the lower limit of pressure at nodes i and j.
$Q_{i,t}^{\mathrm{EL}}$	Load reactive power of node i at time t.
$\overline{Q}_{\mathrm{g}}, \underline{Q}_{\mathrm{g}}$	Upper and lower limits of the reactive power output of the g^{th} generator.
$\overline{q}_{\mathrm{NG},i}, \underline{q}_{\mathrm{NG},i}$	Upper and lower limits of the natural gas supply flow rate of the gas well in node i.
$q_{i,t}^{\mathrm{GL}}$	Gas load on node i at time t.
RU_{g}, RD_{g}	Maximum active power rise and decrease of the generator.
$\overline{T}_{\mathrm{g}}, \underline{T}_{\mathrm{g}}, \overline{T}_{\mathrm{h}}, \underline{T}_{\mathrm{h}}$	Supply and return temperature limit.
$\overline{V}_i, \underline{V}_i$	Upper and lower limits of the allowable value of node i voltage.
θ_{ij}	Voltage phase angle difference between nodes i and j.
β_{com}	Coefficient of the compressor.
μ_{e}, μ_{g}, μ_{h}	Loss rate of EES, GES and HES.
η_{CHP}, η_{HE}, η_{T}, η_{HR}, η_{AC}, η_{P2G}, η_{EC}	Efficiency of CHP, HE, T, HR, AC, P2G, EC.
η_{ech}, η_{edis}	Charge and discharge efficiency of EES.
η_{gch}, η_{gdis}	Injection and extraction efficiency of GES.
η_{hch}, η_{hdis}	Endothermic and exothermic efficiency of HES.
φ_{CHP}	Thermoelectric ratio of CHP.

D. Variables

$B_{s,1,i}$, $B_{s,2,i}$	Investment cost and maintenance cost in the lifetime of the i^{th} and the s^{th} MES.
$B_{s,1}$, $B_{s,2}$	Investment cost and run maintenance cost of the s^{th} MES.
$D_{s,\mathrm{dis}}$	Depth of discharge of the s^{th} MES.
$E_{s,\mathrm{e}}$	Nominal capacity of the s^{th} MES.
E_t^{EES}	Storage capacity of EES on node i at time t.
E_t^{GES}	Storage capacity of GES on node i at time t.
$E_{\mathrm{loss},t}$, $H_{\mathrm{loss},t}$	Power loss and heat loss at time t.
$E_{ij,t}$	Pipe storage in pipe ij at time t.
F_1	Annual system operating costs.
F_2	Sum of the annual cost of all types of MES.
$F_{i,t}^{\mathrm{GES,in}}$, $F_{i,t}^{\mathrm{GES,out}}$	Injection and extraction flow of node i at time t.
G_t, E_t	Gas and electricity consumption at time t.
$G_{s,t}$	Total output of the system of the s^{th} energy.
$H_{i,t}^{\mathrm{HES}}$	Storage capacity of HES on node i at time t.
$h_{i,t}^{\mathrm{L}}$	Consumption quantity of heat in node i at time t.
K	Number of configurations for the s^{th} MES.
$N_{i,\mathrm{HES}}$	Number of HES by node i.
$N_{i,\mathrm{EES}}$	Number of EES by node i.
$N_{i,\mathrm{GES}}$	Number of GES by node i.
N_s	Theoretical cycle number of the s^{th} MES.
n_s	Cycle number of the s^{th} MES.
P_{E}	Consumption of electricity.
P_{G}	Consumption of gas.
$P_{ij,t}$	Active power of the line between nodes i and j at time t.
$P_{g,t}$	Active power of the g^{th} generator at time t.
$P_{i,t}^{\mathrm{w}}$	Wind power active power of node i at time t.
$p_{i,t}$, $p_{j,t}$	Pressure values of the first and last nodes i and j at time t.
$P_{s,\mathrm{e}}$	Rated power of the charge and discharge of the s^{th} MES.
$\tilde{P}_{ij,t}$	Average pressure of pipe ij at time t.
$P_{\mathrm{ML,G},t}$, $P_{\mathrm{ML,E},t}$	The gas and electricity consumption in time t in the medium-long-term market.
$P_{\mathrm{SM,G},t}$, $P_{\mathrm{SM,E},t}$	The gas and electricity consumption in time t in the spot market.
$P_{\mathrm{cw},t}$	Amount of abandoned wind at time t.
$P_{i,t}^{\mathrm{EES,in}}$, $P_{i,t}^{\mathrm{EES,out}}$	Charging and discharging power of the node i at time t.
$Q_{ij,t}$	Reactive power of the line between nodes i and j at time t.
$Q_{g,t}$	Reactive power of the g^{th} generator at time t.
$q_{j,t}^{\mathrm{g}}$	Mass flow of hot water in pipe j at time t.
$q_{i,t}^{\mathrm{HES,in}}$, $q_{i,t}^{\mathrm{HES,out}}$	Endothermic and exothermic heat of node i at time t.

$\tilde{q}_{ij,t}$	Average flow rate flowing through pipe ij at time t.
$q_{ij,t}^{\mathrm{in}}, q_{ij,t}^{\mathrm{out}}$	First natural gas injection flow and the end natural gas output flow of pipe ij at time t.
$q_{i,t}^{\mathrm{NG}}$	Output of the gas source at time t.
$q_{i,t}^{\mathrm{P2G}}$	P2G supply flow rate at node i at time t.
$q_{i,t}^{\mathrm{CHP}}$	Natural gas flow consumed by the CHP at node i at time t.
$q_{i,t}^{\mathrm{GB}}$	Natural gas flow consumed by the GB at node i at time t.
T_s	Life cycle of the s^{th} MES.
$T_{j,t}^{\mathrm{O}}$	Hot water outlet temperature in pipe j at time t.
$T_{k,t}^{\mathrm{I}}$	Hot water inlet temperature in pipe k at time t.
$T_{i,t}^{\mathrm{g}}$	Water supply temperature in node i at time t.
$T_{i,t}^{\mathrm{h}}$	Water return temperature in node i at time t.
$V_{i,t}$	Node voltage of node i at time t.
y_s	Year of the s^{th} energy storage use.
$\lambda_{\mathrm{e},1}$, $\lambda_{\mathrm{e},2}$, $\lambda_{\mathrm{e},3}$	Input power distribution ratio.
$\lambda_{\mathrm{g},1}$, $\lambda_{\mathrm{g},2}$	Input natural gas distribution ratio.

I. Introduction

An IES involves energy production, conversion and coordination, which is conductive to promoting the efficient use of energy [1]. Due to the coupling and complementation of different energy forms in the IES [2], [3], the system itself has a certain flexibility and reserve value. When the operation scene changes, the system can change the operating mode of the coupled device to adapt to the requirements of the scene. When the energy supply is insufficient, the system line pack can also provide an amount of spare energy supply demand [4]. However, as renewable energy becomes increasingly available, the system supply uncertainty also increases, which complicates the system's economic operation and energy utilization [5]. As a time conversion device for energy, the storage of power, gas and heat can smooth the fluctuations of renewable energy and improve the economy and energy utilization efficiency of the IES [6]. Therefore, aiming at the system uncertainty caused by renewable energy access, we consider the economic value of the spare capacity of the system itself and the use of system reserve value to improve the economy, the comprehensive planning of multiple types of reserve energy storage from the level of the IES is of great significance to fully use the flexibility and reserve value of the system. It is also beneficial to improve system economy and energy utilization efficiency.

The integrated planning method of MES is closely related to the IES planning research. At present, most studies on IES planning focus on the modeling and planning of the "source" and "network" of the MES with different backgrounds and components. On the "source" side, existing studies have been able to establish planning models that consider electrical/thermal/gas multi-energy coupling based on the energy hub [7]–[9]. In addition, based on the running of the typical scenario [10], such planning models can consider the differential energy requirements of multiple stakeholders [11] and the energy storage properties of cold, heat and power [12]. Aiming at improving energy utilization efficiency [13] and operation costs [14], the optimal bilevel programming model for system configuration and day-ahead operations are established, and a regional integrated energy station planning method is proposed [15]. In terms of source and network, according to the heating period and cooling period [16], one can establish the entire energy transportation model [17], introduce the evaluation index and method of energy characterization [18], consider the day-ahead dispatch and market uncertainty [19], [20], and propose a multi-region IES collaborative planning method [21]. At present, planning and research on the IES are mostly based on different benefit objectives to determine equipment selection, equipment capacity and the operation strategy of the system and rarely involve configuration methods of the MES [22], [23]. Most studies are based on the battery model considering the absorption of wind and power of the system and the configuration of optimal economic operations for energy storage [24]. The research on MES is also primarily concerned with optimization configuration methods of hybrid energy storage, such as batteries and supercapacitors. The profit strategies of cold storage, heat storage, electricity storage and mixed energy storage under the situation of the CCHP and electric refrigeration's coordinated operations are studied in [25]. A two-layer optimization model to schedule and plan cold storage, heat storage and electrical energy storage is established. It can be seen that the existing research not only lacks the configuration research of MES, but also only considers the cost of investment and operations when configuring MES, and lacks consideration of other values.

For the insufficient research on site selection and capacity determination, this paper studies the optimal MES configuration of electricity, gas and heat storage in the IES in terms of system reserve value, based on the IES with renewable energy, considering the reserve value of the system. As an important hub of the IES [26], energy stations connect power networks, gas networks, and thermal networks via CCHP with other energy coupling equipment. The Energy station operation mode has a great effect on the reserve value of the entire system [27]. Therefore, when studying the MES configuration method, this paper considers the reserve values of both the energy subsystem and energy station. The main technical contributions of this paper are as follows:

1) Regarding MES configuration, we consider the system operation method and the value of the system reserve and propose a two-stage energy storage, gas storage and heat storage configuration method. Considering the reserve value of the system and system operation mode, it is beneficial to fully exploit the flexibility and reserve value of the system.

2) Based on the MES configuration method of the IES considering the system reserve value, the effects of different reserve values on multiple types of energy storage configuration are analyzed in different scenarios, such as the changes of the reserve value, coupling degree and system supply capacity.

The remainder of this paper is structured as follows. Section II presents basic assumptions about the operating mechanism of the reserve market and establishes the system reserve value model. Section III establishes the IES model, including the energy station. In Section IV, a two-stage MES configura-

tion model, considering the reserve value of the system, is established, which includes the location optimization model and capacity optimization model, and the solution process is provided. Section V analyzes through examples the effects of factors, such as whether to consider the reserve value of energy stations, the method to participate in the reserve market, and whether to consider the energy stations, on the configuration result. The effectiveness of the proposed method is also verified. Section VI summarizes the main conclusions of this paper. Section VII provides a brief outlook for the future in this area of research.

II. Basic Assumption

A. Reserve Market Operation Mechanism

As shown in Fig. 1, the operating mechanism of the reserve market assumed in this paper includes the energy contract market, a balancing mechanism, and settlement. The trading volume of the contract market accounts for the majority of the total volume, including medium- and long-term contracts and spot contracts. The remaining unbalanced trading volume is solved through the balancing mechanism in the reserve service market. Medium- and long-term contracts are allowed to be signed several years in advance and are primarily completed by bilateral organizations, while short-term spot transactions are primarily completed through centralized matching. After trading activity is stopped, the dispatching agency arranges the scheduling plan according to the load prediction, day-ahead safety check, unit start and stop arrangement, etc. One hour before the actual operation, the demand for reserve service is obtained through the balancing mechanism to solve the constraint problem of the energy system and maintain the balance of supply and demand of the system. After dispatching according to the price of the reserve service, the unbalanced settlement is made according to the actual energy supply curve of the unit. The market subject that provides the reserve service will obtain the corresponding profit [28].

Energy station and energy subsystem units arrange day-ahead dispatching plans according to the transaction value of medium- and long-term contracts and spot contracts. By reserving the capacity to participate in the ancillary services market, the balance between supply and demand of the system can be maintained through the balance mechanism, and a certain profit can be simultaneously obtained. Therefore, the reserve value of the system can be measured by the reserved capacity of the system units and energy stations (including actual participation and nonparticipation).

B. System reserve value Model

The system reserve value model in this paper includes the capacity opportunity cost and reserve energy cost. The capacity opportunity cost refers to the loss of power generation profit due to the lost opportunity to participate in the energy market because of the reserved capacity during a short run of the system. The reserve energy cost refers to the cost of actually participating in the short-term reserve market. Combined with the distribution network characteristics of the IES in this paper, the system reserve value is shown in (1):

$$R_{s,t} = (\overline{G}_{s,t} - G_{s,t}) \cdot (C_{s,t} + D_{s,t}) \tag{1}$$

III. Power-gas-heat Integrated Energy System Model

A. Energy Stations Model

Energy stations serve as energy hubs for EPS, NGS and DHS. An energy station's normal operation is restricted by the states of the EPS, NGS and DHS. The change of the station's running state also causes changes to the entire system with EPS, NGS and DHS.

The energy station constructed in this paper includes CHP, T, HE, HR, P2G, EC, and AC. The source-load supply relationship of the EPS, NGS and DHS is connected through the equipment in these energy stations. The energy balance equation is:

$$\begin{bmatrix} L_{\mathrm{e}} \\ L_{\mathrm{g}} \\ L_{\mathrm{h}} \\ L_{\mathrm{c}} \end{bmatrix} = \begin{bmatrix} \lambda_{\mathrm{e},1} & \lambda_{\mathrm{g},1}\eta_{\mathrm{T}}\eta_{\mathrm{CHP}}(1+\phi_{\mathrm{CHP}})^{-1} \\ \lambda_{\mathrm{e,e}}\eta_{\mathrm{P2G}} & \lambda_{\mathrm{g},2} \\ 0 & \lambda_{\mathrm{g},1}\eta_{\mathrm{HE}}\phi_{\mathrm{CHP}}\eta_{\mathrm{CHP}}(1+\phi_{\mathrm{CHP}})^{-1} \\ \lambda_{\mathrm{e},3}\eta_{\mathrm{EC}} & \lambda_{\mathrm{g},1}\eta_{\mathrm{AC}}\eta_{\mathrm{HR}}\eta_{\mathrm{HE}}\phi_{\mathrm{CHP}}\eta_{\mathrm{CHP}}(1+\phi_{\mathrm{CHP}})^{-1} \end{bmatrix} \begin{bmatrix} P_{\mathrm{E}} \\ P_{\mathrm{G}} \end{bmatrix} \tag{2}$$

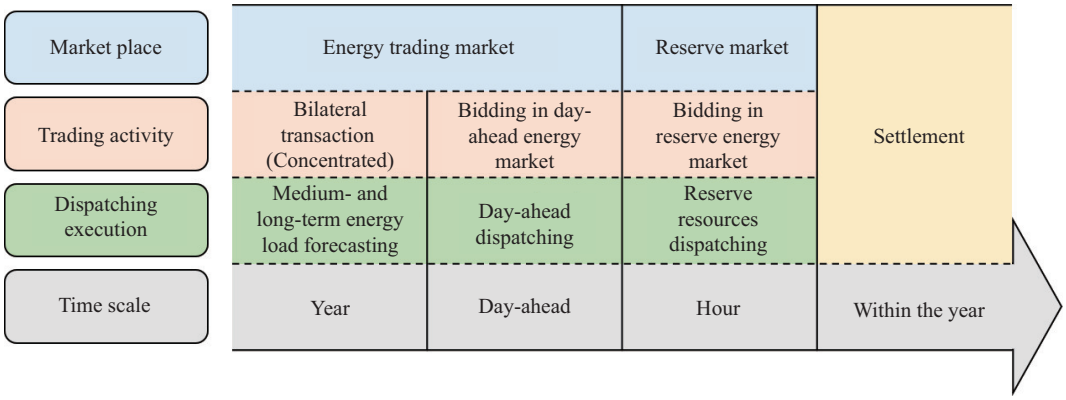

Fig. 1. Reserve market operation mechanism.

B. EPS Model

The EPS model includes the power balance constraint, node voltage constraint, three-phase power flow constraint, line power constraint, generator set output constraint and generator set climbing constraint [29].

$$\sum_{j\in\Omega_l^i} P_{ij,t} = \sum_{g\in\Omega_{\mathrm{G}}^i} P_{g,t} + P_{i,t}^{\mathrm{w}} + P_{i,t}^{\mathrm{CHP}} + P_{i,t}^{\mathrm{EES,in}} - P_{i,t}^{\mathrm{EES,out}} - P_{i,t}^{\mathrm{P2G}} - P_{i,t}^{\mathrm{EL}} \tag{3}$$

$$\sum_{j\in\Omega_l^i} Q_{ij,t} = \sum_{g\in\Omega_{\mathrm{G}}^i} Q_{g,t} - Q_{i,t}^{\mathrm{EL}} \tag{4}$$

$$\underline{V}_i \le V_{i,t} \le \overline{V}_i \tag{5}$$

$$\sum_{j\in\Omega_l^i} P_{ij,t} - V_{i,t}\sum_{j\in\Omega_l^i} V_{j,t}\left(G_{ij}\cos\theta_{ij} + B_{ij}\sin\theta_{ij}\right) = 0 \tag{6}$$

$$\sum_{j\in\Omega_l^i} Q_{ij,t} - V_{i,t}\sum_{j\in\Omega_l^i} V_{j,t}\left(G_{ij}\sin\theta_{ij} - B_{ij}\cos\theta_{ij}\right) = 0 \tag{7}$$

$$-\overline{P}_{ij} \le P_{ij,t} \le \overline{P}_{ij} \tag{8}$$

$$\underline{P}_{\mathrm{g}} \le P_{g,t} \le \overline{P}_{\mathrm{g}} \tag{9}$$

$$\underline{Q}_{\mathrm{g}} \le Q_{g,t} \le \overline{Q}_{\mathrm{g}} \tag{10}$$

$$P_{g,t} - P_{g,t-1} \le RU_g \tag{11}$$

$$P_{g,t-1} - P_{g,t} \le RD_g \tag{12}$$

C. NGS Model

The NGS model includes the pipeline flow constraint, gas source point constraint, flow balance constraint, compressor constraint, line pack constraint and node pressure constraint [30].

$$\tilde{q}_{ij,t}|\tilde{q}_{ij,t}| = C_{ij}^2(p_{i,t}^2 - p_{j,t}^2) \tag{13}$$

$$\tilde{q}_{ij,t} = 2^{-1}(q_{ij,t}^{\mathrm{in}} - p_{ij,t}^{\mathrm{out}}) \tag{14}$$

$$\underline{q}_{\mathrm{NG}.i} \le q_{i,t}^{\mathrm{NG}} \le \overline{q}_{\mathrm{NG}.i} \tag{15}$$

$$0 = q_{i,t}^{\mathrm{NG}} + \sum_{i\in\Omega_j}\tilde{q}_{ij,t} + q_{i,t}^{\mathrm{P2G}} + F_{i,t}^{\mathrm{GES,out}} - F_{i,t}^{\mathrm{GES,in}} - q_{i,t}^{\mathrm{GL}} - q_{i,t}^{\mathrm{CHP}} \tag{16}$$

$$p_{j,t} \le \beta_{\mathrm{com}} p_{i,t} \tag{17}$$

$$E_{ij,t} = M_{ij}\tilde{P}_{ij,t} \tag{18}$$

$$\tilde{P}_{ij,t} = 2^{-1}(p_{i,t} + p_{j,t}) \tag{19}$$

$$E_{ij,t} = E_{ij,t-1} + q_{ij,t}^{\mathrm{in}} - q_{ij,t}^{\mathrm{out}} \tag{20}$$

$$\underline{p}_i \le p_{i,t} \le \overline{p}_i \tag{21}$$

D. DHS Model

Steam and hot water are commonly used as heat carriers in thermal systems. Considering a heat network as a fluid network, the node flow balance, node power fusion, load access characteristics, water supply and return temperature constraints, and heat transfer characteristics of the pipe segments are considered [31].

$$\sum_{j\in S_i^{\mathrm{pipe}+}} q_{j,t}^{\mathrm{g}} = \sum_{k\in S_i^{\mathrm{pipe}-}} q_{k,t}^{\mathrm{g}} \tag{22}$$

$$\sum_{j\in S_i^{\mathrm{pipe}+}} T_{j,t}^{\mathrm{O}} q_{j,t}^{\mathrm{g}} = T_{k,t}^{\mathrm{I}} \sum_{k\in S_i^{\mathrm{pipe}-}} q_{k,t}^{\mathrm{g}} \tag{23}$$

$$h_{i,t}^{\mathrm{L}} = c q_{i,t}^{\mathrm{g}}(T_{i,t}^{\mathrm{g}} - T_{i,t}^{\mathrm{h}}) \tag{24}$$

$$\underline{T}_{\mathrm{g}} \le T_{i,t}^{\mathrm{g}} \le \overline{T}_{\mathrm{g}} \tag{25}$$

$$\underline{T}_{\mathrm{h}} \le T_{i,t}^{\mathrm{h}} \le \overline{T}_{\mathrm{h}} \tag{26}$$

$$T_{\mathrm{e}} = (T_{\mathrm{a}} - T_s)x(Rc\rho f)^{-1} + T_s \tag{27}$$

IV. Optimal Configuration Model of Multitype Energy Storage Considering the System Reserve Value

A. MES Location Model

1) Objective Function of the Location Model

In the objective function, the electric loss of the EPS [17], heat loss of the DHS [21], operating cost of the system, value of the system reserve and loss of curtailment are considered as follows.

$$\min F_1 = \sum_{t=1}^{\mathrm{T}}\Big(C_{\mathrm{e},t}E_{\mathrm{loss},t} + C_{\mathrm{h},t}H_{\mathrm{loss},t} + C_{\mathrm{ML,G}}P_{\mathrm{ML,G},t} + C_{\mathrm{SM,G},t}P_{\mathrm{SM,G},t} + C_{\mathrm{ML,E}}P_{\mathrm{ML,E},t} + C_{\mathrm{SM,E},t}P_{\mathrm{SM,E},t} - \sum_s R_{s,t} + C_{\mathrm{ew}}P_{\mathrm{cw},t}\Big) \tag{28}$$

2) Constraint of the Location Model

The power storage, gas storage and heat storage participate in system operations by switching charging and discharging modes [32]. The constraint of the mathematical model of EES is expressed as follows:

$$E_{i,t}^{\mathrm{EES}} = (1-\mu_{\mathrm{e}})E_{i,t-1}^{\mathrm{EES}} + \left(P_{i,t}^{\mathrm{EES,in}}\eta_{\mathrm{ech}} - P_{i,t}^{\mathrm{EES,out}}\eta_{\mathrm{edis}}^{-1}\right)\Delta t \tag{29}$$

$$E_{i,1}^{\mathrm{EES}} = E_{i,24a}^{\mathrm{EES}} \quad a = 1,2,\cdots,365 \tag{30}$$

$$\underline{E}_{\mathrm{EES}} \times N_{i,\mathrm{EES}} \le E_{i,t}^{\mathrm{EES}} \le \overline{E}_{\mathrm{EES}} \times N_{i,\mathrm{EES}} \tag{31}$$

The constraint of the mathematical model of GES is expressed as follows:

$$E_{i,t}^{\mathrm{GES}} = (1-\mu_{\mathrm{g}})E_{i,t-1}^{\mathrm{GES}} + \left(F_{i,t}^{\mathrm{GES,in}}\eta_{\mathrm{gch}} - F_{i,t}^{\mathrm{GES,out}}\eta_{\mathrm{gdis}}^{-1}\right)\Delta t \tag{32}$$

$$E_{i,1}^{\mathrm{GES}} = E_{i,24a}^{\mathrm{GES}} a = 1,2,\cdots,365 \tag{33}$$

$$\underline{E}_{\mathrm{GES}} \times N_{i,\mathrm{GES}} \le E_{i,t}^{\mathrm{GES}} \le \overline{E}_{\mathrm{GES}} \times N_{i,\mathrm{GES}} \tag{34}$$

The constraint of the mathematical model of HES is expressed as follows:

$$H_{i,t}^{\mathrm{HES}} = (1-\mu_{\mathrm{h}})H_{i,t-1}^{\mathrm{HES}} + \left(Q_{i,t}^{\mathrm{HES,in}}\eta_{\mathrm{hch}} - Q_{i,t}^{\mathrm{HES,out}}\eta_{\mathrm{hdis}}^{-1}\right)\Delta t \tag{35}$$

$$E_{i,1}^{\mathrm{HES}} = E_{i,24a}^{\mathrm{HES}} \quad a = 1,2,\cdots,365 \tag{36}$$

$$\underline{H}_{\mathrm{HES}} \times N_{i,\mathrm{HES}} \le H_{i,t}^{\mathrm{HES}} \le \overline{H}_{\mathrm{HES}} \times N_{i,\mathrm{HES}} \tag{37}$$

The quantity constraints of the electricity, gas and heat storage are as follows:

$$\sum_i N_{i,\mathrm{EES}} \le \bar{N}_{\mathrm{EES}} \tag{38}$$

$$\sum_i N_{i,\mathrm{GES}} \le \bar{N}_{\mathrm{GES}} \tag{39}$$

$$\sum_i N_{i,\mathrm{HES}} \le \bar{N}_{\mathrm{HES}} \tag{40}$$

B. MES Capacity Optimization Model

1) Cycle Life Loss Model

Temperature and charging and releasing energy cycle times, among other factors, affect the cycle life of electricity storage, gas storage, and heat storage. In this paper, energy storage cycle life refers to the service life of electricity storage, gas storage and heat storage under certain charging and discharging efficiencies. The depth of discharge directly affects energy storage cycle life and is denoted as $D_{s,\mathrm{dis}}$. In this paper, the effects of energy depth and cycle times on cycle life are considered.

According to [33], the effect of the depth of the discharge energy on cycle life is expressed by a polynomial function of order 4, and the functional relationship is shown in (41).

$$N_s(D_{s,\mathrm{dis}}) = a_s D_{s,\mathrm{dis}}^4 + b_s D_{s,\mathrm{dis}}^3 + c_s D_{s,\mathrm{dis}}^2 + d_s D_{s,\mathrm{dis}} + e_s \tag{41}$$

Energy storage operating conditions can be considered to be a series of linear combinations of charging and discharging cycles with different discharge depths. The operating condition is decomposed into several operating conditions with different discharge depths, and the cycle life of energy storage in each condition after decomposition is calculated. Then, according to the cycle times of energy storage in each corresponding working condition, the life loss of the energy storage cycle can be directly calculated by linear superposition. The cycle life loss of energy storage in operations can be calculated according to (39):

$$L_s = \sum_{D_{s,\mathrm{dis}}=0}^{1} \frac{n_s}{N_s(D_{s,\mathrm{dis}})} \tag{42}$$

For each $D_{s,\mathrm{dis}}$ between 0–1, there is a corresponding number of cycles $N_s(D_{s,\mathrm{dis}})$ and the number of cycles n_s that appear. The corresponding $n_s/N_s(D_{s,\mathrm{dis}})$ are calculated and summed through (42). When $L_s = 1$, the energy storage life is considered exhausted and must be replaced.

The energy charge and release cycle times of the energy storage and the corresponding release energy depth are calculated by the rain flow counting method. The cycle life loss in the operation process is obtained from (41) and (42).

2) Full-Life-Cycle Cost Model

The energy storage life cycle cost refers to the total cost of energy storage investment, maintenance and guarantee during the life cycle. The entire life cycle cost of energy storage includes investment cost and the operation and maintenance costs.

The primary investment cost is a function of the rated capacity of energy storage and rated power and is expressed as:

$$B_{s,1} = C_{s,\mathrm{e}} E_{s,\mathrm{e}} + C_{s,\mathrm{p}} P_{s,\mathrm{e}} \tag{43}$$

The energy storage operation and maintenance costs are a function of the rated capacity of the energy storage, related to its operation cycle, and expressed as:

$$B_{s,2} = \sum_{t=1}^{T_s} C_{s,\mathrm{m}} P_{s,\mathrm{e}} \left(\frac{1+i_\mathrm{r}}{1+d_\mathrm{r}}\right)^{y_s} \tag{44}$$

3) Objective Function of the Capacity Optimization Model

According to the energy storage charging and releasing strategy, which is solved by the location model of energy storage in the first stage and the relationship between energy storage cycle life and energy release depth, we know that a larger capacity connected to the energy storage corresponds to a longer energy storage service life for a certain number of cycles per day. However, given the high cost per unit of energy storage capacity, if energy storage with excessive capacity is configured simply to extend its service life, its primary investment cost will significantly increase. Although a higher capacity will extend the service life, the total investment and maintenance cost will also increase. Therefore, it is necessary to further optimize energy storage capacity based on a comprehensive consideration of the energy storage life cycle cost and service life to maximize the economy of the electricity, gas and heat storage.

In this paper, the full-life cycle cost of MES is allocated to each year of the life cycle. To minimize the sum of the annual costs of all types of energy storage within the service life of the energy storage, the energy storage capacity is optimized. The target function expression is as follows:

$$\min F_2 = \sum_s \sum_{i=1}^{k} \frac{B_{s,1,i} + B_{s,2,i}}{T_{s,i}} \tag{45}$$

C. Model Solving

Based on the reserve market mechanism of the IES including energy stations, this paper establishes a two-stage MES optimization configuration model for the IES to optimize the site selection and capacity determination of batteries, heat storage tanks, gas storage tanks, etc. The solution process is shown in Fig. 2. In the first step, wind power and load data are input, a random scene is generated through Latin cube sampling, and then a fuzzy c-means clustering method is used for scene reduction. Second, for the site selection model to minimize the system operating cost, behaving as a mixed integer nonlinear programming problem, GAMS software is

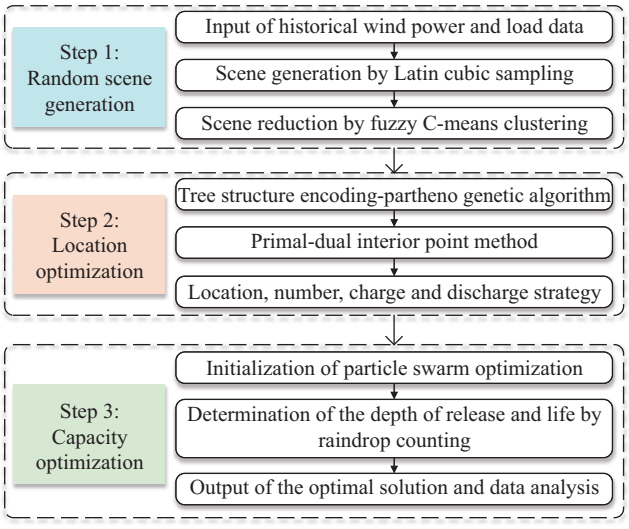

Fig. 2. Solution flow.

used to obtain both the location of energy storage and a charging strategy by combining the parthenogenetic algorithm and primal-dual interior point method encoded by the tree structure. The third step is to obtain the capacity of the MES by using the particle swarm algorithm of the nested energy storage life calculation on MATLAB software. This method realizes the solution of nonlinear models to minimize the investment and maintenance costs of the MES in the system.

V. Results

A. Basic Data

This paper is based on using the MATLAB and GAMS platforms on a Win10 operating system, i7CPU, 2.20 GHz processor environment for the simulation and optimization analysis. The structure of the IES with renewable energy discussed in the example is shown in Fig. 3. The IES is composed of three main parts: the modified IEEE 14-node EPS, the 11-node NGS [34], and the modified DNS based on [27]. The energy flow is conducted through the regional energy station for energy coupling and energy interaction. The regional energy station is located at the coupling node formed by 4 nodes of the EPS, 7 nodes of the NGS, and 8 nodes of the DHS. We convert the natural gas flow through the calorific value to the power per unit of kW. The energy price of the system is referred to the peak-valley price in [35]. The equipment parameters in the energy station are referenced in [36]. The main relevant operating condition constraints include:

- In the EPS, the per-unit voltage range is 0.95–1.05
- In the NGS, the minimum pressure is 22.5 mbar; the upper limit of pipeline 12–14 flow is 150 m^3/h;
- In the DHS, the maximum mass flow allowed in the pipeline is 1.6 kg/s, the upper and lower limits of the water supply temperature are 70°C and 69°C, respectively, and the upper and lower limits of the return water temperature are 30°C and 29°C, respectively.

B. Result Analysis

1) Analysis of the Configuration Results

S1: MES-integrated configuration considering the energy station and short-term system reserve value

First, based on the data from a location in Germany [37], the method of Step 1 in Section IV-C is used. The wind power, power load, gas load and heat load of 8,760 hours per year are shown in Fig. 4. The 24-h price is adopted in the reserve market. Fig. 5 shows the price of electricity and natural gas in the reserve market. The price of electricity has a peak-valley form. The price of natural gas is a fixed value. Heat reserve decides to use the reserve electricity price or reserve gas price according to the input of heating equipment.

Then, based on the wind power, electric load, gas load and heat load power, the model of Section III and Section IV-A uses the method of Step 2 in Section IV-C to obtain the location, quantity and charging and releasing energy strategy of EES, GES, and HES.

Finally, based on the above results and the model in Section IV-B, the capacities of EES, GES and HES are obtained by using the method of Step 3 in Section IV-C. The convergence is shown in Fig. 6.

According to Fig. 6, after approximately 280 iterations, the particle swarm reached convergence and obtained the final configuration scheme.

We convert the mass flow rate of natural GES into a success rate unit according to the calorific value of natural gas. The solution results are shown in Table I.

Due to the relatively large fluctuation of the electric load in Fig. 4, there is more demand for EES charging and discharging. Even if the P2G in the energy station can convert

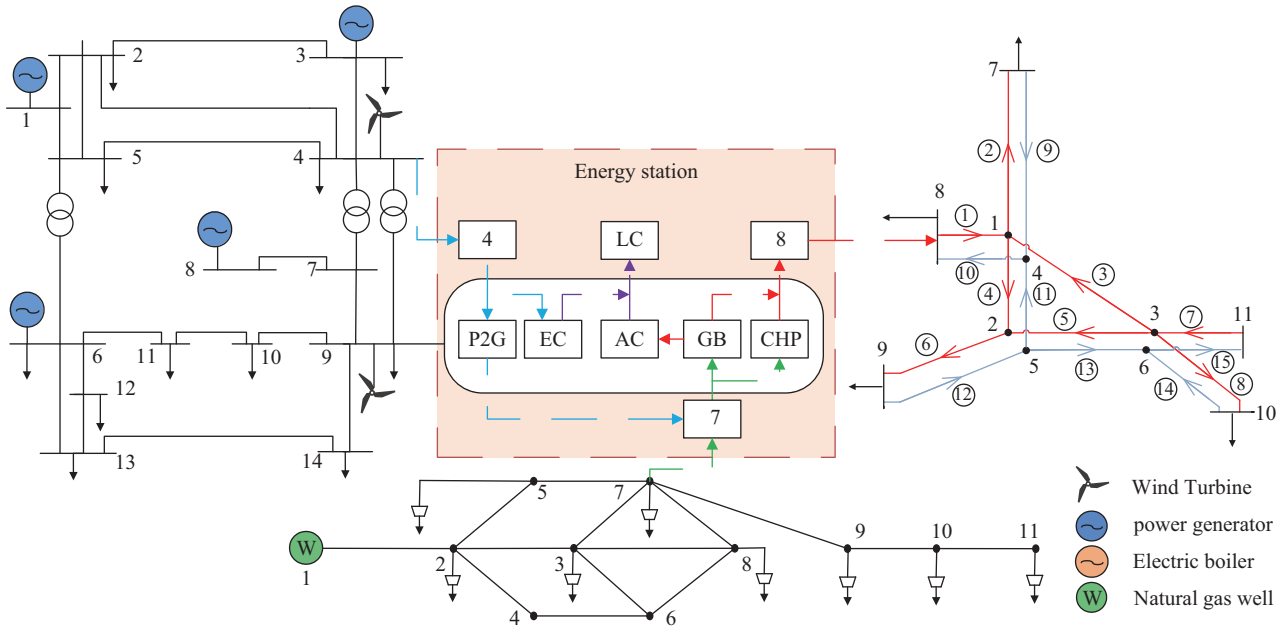

Fig. 3. Integrated energy system.

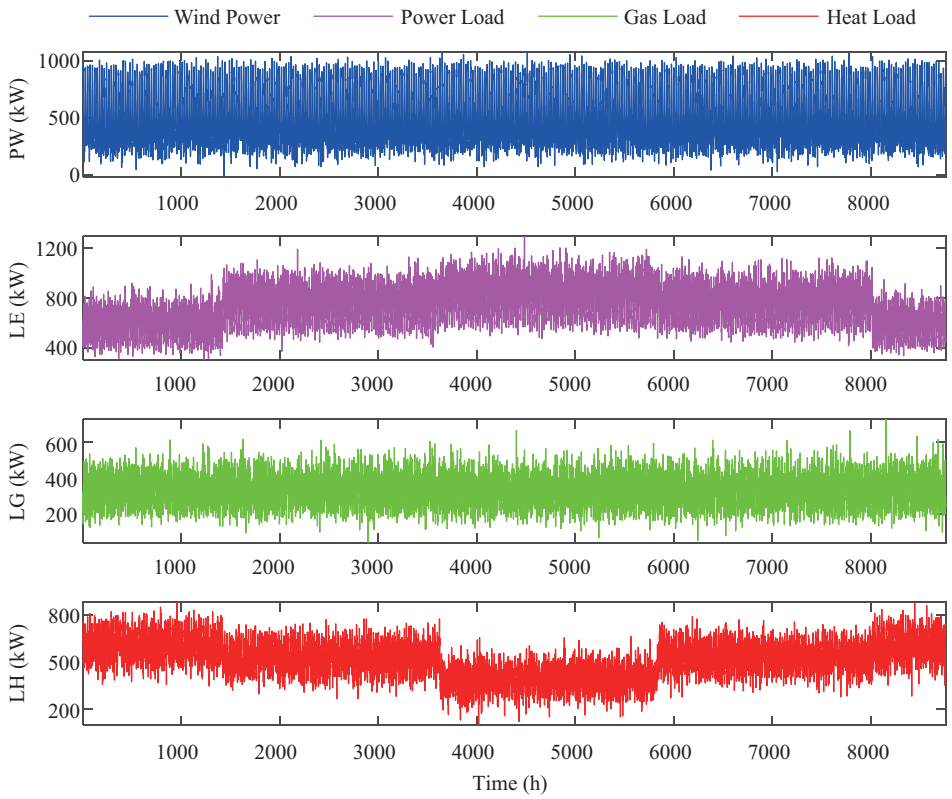

Fig. 4. Scene data graph.

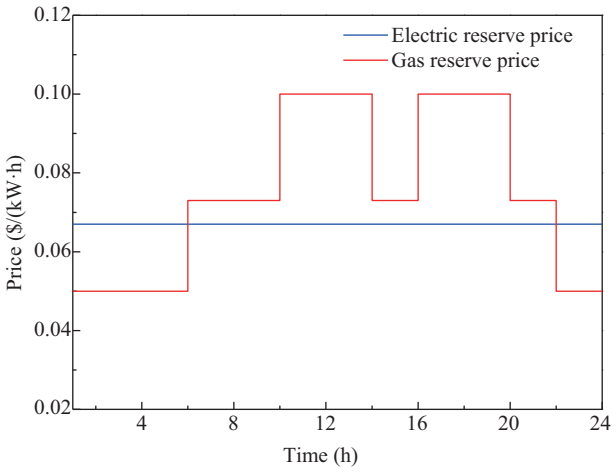

Fig. 5. Short-term reserve service price.

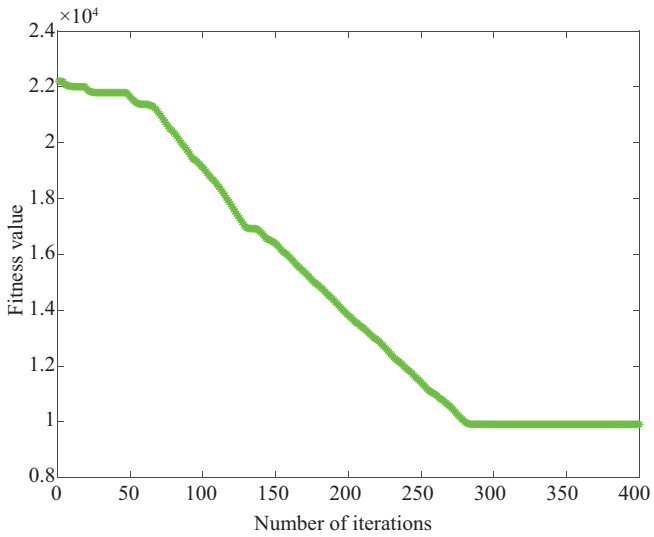

Fig. 6. Iterative convergence.

electric energy into natural gas for storage, the electric load fluctuation must be balanced in a timely way due to the fast dynamic characteristics of the power system. Due to the power flow constraints, some node loads on the EPS far away from the energy stations still need a timely supply of electric energy storage. Therefore, in Table I, EPS node 2 and node 11 are connected with the EES. The configured EES capacity is also large. The fluctuation of the electric load leads to frequent charging and discharging, and the operating life of the EES is only 1.87 and 1.75 years. Excepting seasonal differences, the fluctuation of the gas load and heat load curve in Fig. 4 is relatively small. The NGS system itself has certain attributes of the line pack. The DHS has certain temperature delay characteristics. The requirement of the gas and heat supply is not as high as that of electricity, and the energy station coupling equipment has a certain energy conversion capacity, which can use the surplus electricity to supply gas and heat loads. Therefore, only 9 nodes of the NGS and 2 nodes of the DHS are connected to GES and HES, respectively. The capacity is smaller than that of the EES, the charging and discharging frequency is not particularly frequent, and the service life of the GES and HES is 2.46 and 2.53 years,

TABLE I
RESULT OF THE MES-INTEGRATED CONFIGURATION CONSIDERING THE ENERGY STATION AND SHORT-TERM SYSTEM RESERVE VALUE

s	i	$E_{s,e}$ (kW·h)	$P_{s,e}$ (kW)	y	F_s ($)	F_2 ($)
EES	2	106	15	1.87	34738.64	67962.52
	11	96	10	1.75		
GES	9	128	50	2.46	7585.76	
HES	2	59	10	2.53	25638.12	

respectively. According to Table I, the EES has the highest configuration cost, and most of the expenses are used to invest in the EES. The fluctuations of electric load and the fast dynamic characteristics of the power system leads to the demand of MES in the IES, which is still the main type of electric energy storage.

2) Effect of the System reserve value on the Configuration

S2: MES-integrated configuration without considering the system reserve value

In the model in Section IV-A, the reserve value of the system is not considered, but the system operation cost is only used as the objective function. Then, according to the solution steps of STEP3 in Section IV-C, the configuration results are shown in Table II.

Because the reserve value of the system is not considered, the system loses part of the profit of providing the reserve service during the run time, which results in an increase in running cost. As shown in Fig. 7, for example, with the discharge depth of the electricity, gas and heat storage on the same day in scenes S1 and S2, since no reserve value is reserved for the system in S2, the adjustable range is large. In addition, without considering the impact of the charging and discharging frequency and depth on the system operation during site selection optimization, scenario II has a greater charging and discharging frequency of the MES in scenario S2 than in scenario S1. The charging and discharging curve of scenario S2 is more tortuous, which decreases the cycle life of multiple types of energy storage, especially GES and HES, and increases the investment cost. Therefore, in Table II, the configuration results of EES, GES and HES in scenario S2 are compared with those in scenario S1. The result of access location is identical to that in scenario S1, with a small difference in capacity, but the operating life is relatively decreased, and the annual investment cost is increased.

TABLE II
RESULT OF THE MES-INTEGRATED CONFIGURATION WITHOUT CONSIDERING THE SYSTEM RESERVE VALUE

s	i	$E_{s,e}$ (kW·h)	$P_{s,e}$ (kW)	y	F_2 ($)
EES	2	136	15	1.85	70408.88
	11	92	10	1.71	
GES	9	100	50	2.39	
HES	2	60	10	2.48	

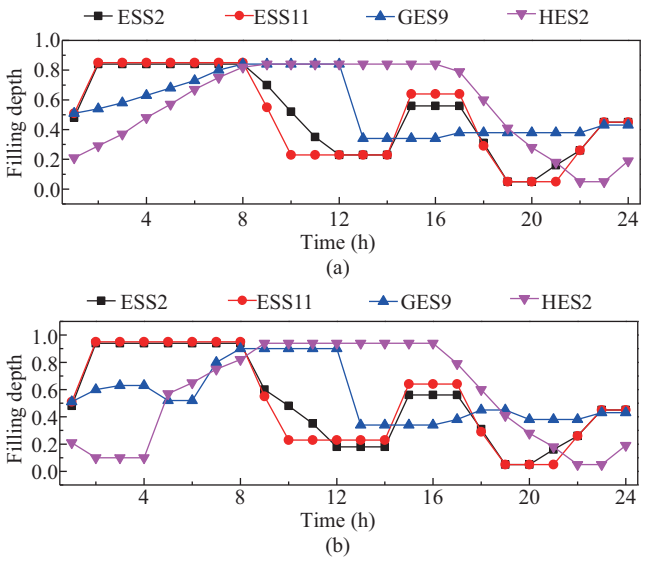

Fig. 7. S1 and S2 scene multi-type discharge depth of energy storage. (a) The filling depth of multi-type energy stroage in S1. (b) The filling depth of multi-type energy stroage in S2.

3) Effect of the reserve value of the Energy Station on MES Configuration

S3: Independent configuration of MES without considering the reserve value of the energy station

Without considering the reserve value of the energy station, other conditions and solution methods are identical to those in S1 in V-B(1). The configuration results are shown in Table III.

TABLE III
RESULT OF THE INDEPENDENT CONFIGURATION OF THE MES WITHOUT CONSIDERING THE ENERGY STATION

s	i	$E_{s,e}$ (kW·h)	$P_{s,e}$ (kW)	y	F_2 ($)
EES	2	116	15	1.85	69402.34
	11	96	10	1.75	
GES	9	100	50	2.40	
HES	2	59	10	2.48	

The alternate capabilities between the EPS, NHS and DHS are primarily realized through energy stations. Without considering the reserve value of the energy station, the reserve value of the system, especially the coupling equipment of the energy station, is not sufficient, the reserve value of the system decreases, and the operating cost increases. Meanwhile, similar to S2, without considering the reserve value of the energy station, the adjustable range of the system increases, the cycle life of S3 MES decreases, and the annual investment cost increases. Therefore, in Table III, even if the installed position of MES does not change compared to S1, the final annual investment cost is $69402.34, which is higher than that of scenario S1.

4) Effect of the Coupling of EPS, NGS, and DHS on MES Configuration

S4: The coupling of the EPS, NGS and DHS is not considered for the independent configuration of each type of energy storage; EES is only configured in the EPS system, GES is only configured in the NGS, and HES is only configured in the DHS. Other conditions and solution methods are identical to those in S1 of V-B(1). The configuration results are shown in Table IV.

EES, GES and HES are independently configured in their respective systems, that is, the interaction between the EPS, NGS, and DHS is ignored. As a result, higher requirements are introduced for the charging and releasing energy of energy

TABLE IV
RESULT OF THE INDEPENDENT CONFIGURATION OF MES WITHOUT CONSIDERING THE ENERGY STATION

s	i	$E_{s,e}$ (kW·h)	$P_{s,e}$ (kW)	y	F_2 ($)
EES	2	136	15	1.85	84026.84
	5	79	10	1.54	
	11	96	10	1.75	
GES	7	51	10	2.86	
	9	128	50	2.23	
HES	2	59	10	2.48	

storage in each subsystem, especially for EES. It is difficult for the independent equipment of the EPS to convert the surplus gas in the NGS into electricity to supply the electric load, so it can only be supplied through EES, which increases the demand for EES. Similarly, the NGS can only store natural gas at lower gas prices through gas storage. Therefore, in Table IV, EES is accessed at node 2, node 5 and node 11 of the EPS, while GES is accessed at node 7 and node 9 of the NGS. One more EES and one more GES are connected than in scene S1. The final annual investment cost is $84,026.84, which is much higher than the investment cost in scenario S1. Thus, whether the EPS, NGS and DHS are coupled significantly affects the position, quantity, capacity and cost of the system energy storage configuration.

5) Effect of the Configuration Scheme on the Annual Investment Cost, System reserve value and Operating Cost in Different Scenarios

The configuration capacity and annual investment cost of electricity storage, gas storage and heat storage in different scenarios (S1, S2, S3 and S4) are compared and analyzed. The results are shown in Fig. 8.

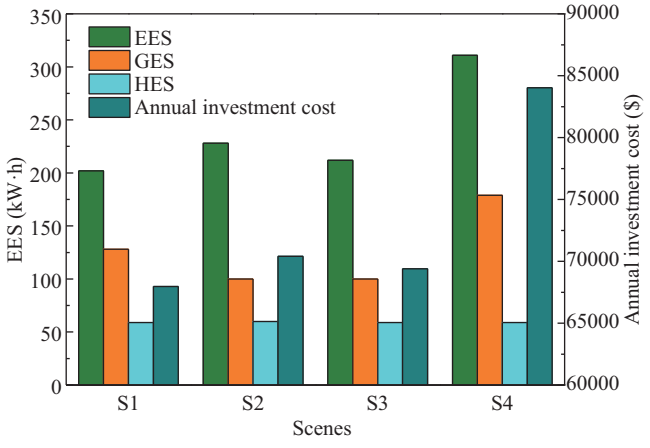

Fig. 8. Comparison of configuration capacity and annual investment cost for different scenarios.

According to Fig. 8, S1 and S2 have high and low electricity storage, gas storage, and heat storage capacity configurations. However, S1 considers the reserve value of the system, which makes the charging and discharging strategy of MES relatively smooth and the service life relatively prolonged. Therefore, S1 has slightly lower annual investment cost than S2. S3 does not consider the reserve value of the energy station, but only part of the reserve value of the system, whose configuration cost is between S1 and S2. Compared with S1, S2 and S3, S4 has the largest capacity of electricity, gas and heat storage; in particular, the electric energy storage is significantly higher than that of S1, so S4 has the highest annual investment cost. Thus, whether the EPS, NGS and DHS couplings are considered in the MES configuration process has a great impact on the annual investment cost of the configuration.

The system reserve value and annual operating cost of different scenario configuration results of S1, S2, S3 and S4 are compared and analyzed, and the results are shown in Fig. 9.

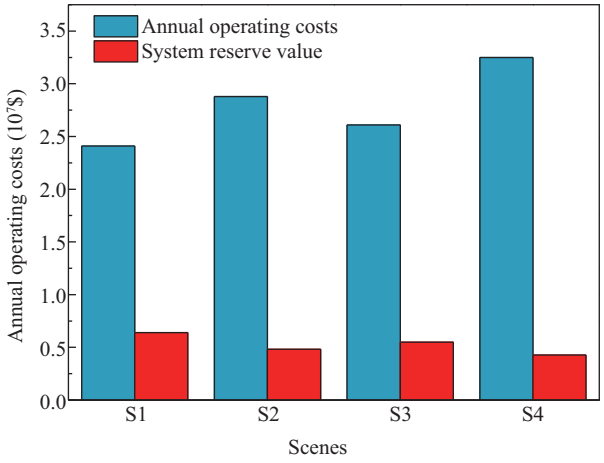

Fig. 9. Comparison of the configuration capacity and annual investment cost for different scenarios.

The coupling effect between the EPS, NGS and DNS was not considered in scenario S4. Compared with scenarios S1, S2 and S3, which consider the coupling effect between systems, S4 has the highest operation cost. Among S1, S2 and S3, S2 does not consider the system reserve value, which is the lowest, and S2 has the highest operation cost because it has not gained any benefit from the reserve market. Compared with S2, S3 considers the reserve value of the system except for energy stations. The reserve value of the system is relatively increased, and some benefits are obtained from the reserve market, so its operating cost is relatively reduced. S1 considers the reserve value of the system, which is the highest, while the reserve market gains, and its operating cost are the lowest. Therefore, MES planning with the system reserve value has certain cost advantages in system operation.

6) Effect of the Method to Participate in Reserve Markets

S5: MES-integrated configuration considering the contractual system reserve value

In order to study the effect of the price of contract reserve services on the MES-integrated configuration, it is assumed that the price of the reserve market is the price of the medium- and long-term reserve service contract signed in advance. All other conditions and solution methods are identical to those of S1 in V-B(1). To fully compare the results of the MES configuration at different contract prices, based on the 24-h price in the reserve market as shown in Fig. 5, and within the range of the maximum and minimum prices of the reserve market price, 6 sets of reserve contract prices are taken. In ascending order, the electricity price is 0.05, 0.06, 0.07, 0.08,

0.09 and 0.10 ($/(kW·h)). Considering the slight fluctuation of the gas price in the reserve market, we take 6 groups of gas reserve contract prices: 0.057, 0.061, 0.064, 0.068, 0.072 and 0.076 ($/(kW·h)). Natural gas is converted to power unit kW according to the calorific value. In ascending order, the reserve contract electricity and gas prices constitute 6 groups of different reserve contract prices. The comparison of configuration results is shown in Fig. 10:

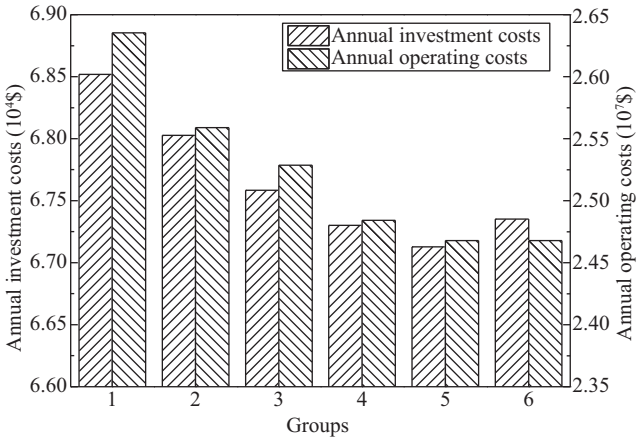

Fig. 10. Comparison of configuration results of different system alternate service contract price.

The system signs medium- and long- term reserve services at different contract prices. Different prices of reserve services directly affect the benefits of the system to provide reserve services and consequently affect the operation mode of the system. When the price of the reserve service rises, the system can profit more from the reserve market, which reduces operating costs and increases the reserve value reserved. According to the relationship between the cycle life of the MES and system reserve in S2, the investment costs of electricity, gas and heat storage will decrease. However, due to the physical constraint of load balance and the constraint of market participation, the increase in reserve service price has a certain limit on the decrease in operating cost and investment cost, and the effect of the decrease is gradually reduced. When the reserve service contract price of group 5 and group 6 is reached, it is no longer decreasing. The reserve value increases, and the remaining adjustable range of the system decreases. To ensure the normal energy supply requirements of the system, the amount of energy storage will increase, which will increase the investment cost of the energy storage configuration of the system. Therefore, as shown in Fig. 10, with the increase in reserve service price, the investment cost of energy storage gradually decreases, and the decrease range becomes increasingly smaller. After reaching the limit, the energy storage investment cost bounces up, while the operating cost gradually decreases and reaches the minimum with the increase in reserve service price.

7) Evaluation of MES configuration results of the IES considering the system reserve value

S6: Assume that the 1-node EPS unit is dismantled due to aging, and the system supply capacity is reduced.

The running situation of the S1, S2, S3 and S4 configuration results is analyzed in the scenario of reduced system supply capacity. The results are shown in Fig. 11.

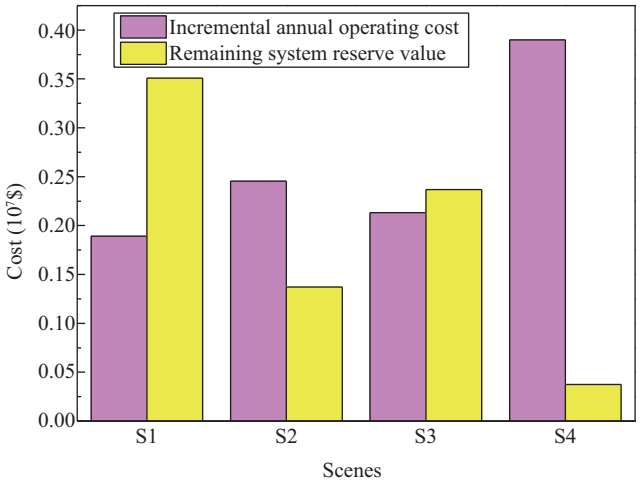

Fig. 11. Comparison of system annual operating costs and remaining system reserve value in S7.

After the removal of the EPS1 nodal unit, the incremental annual operating cost and remaining system reserve value represent the change when the system supply capacity decreases. According to Fig. 11, the coupling effect among the EPS, NGS and DNS was not considered in scenario S4. When the system supply capacity decreases, the energy supply is only obtained from the subsystem interior due to the absence of coupling and complementation among the systems. The annual incremental operating cost is the highest, and the remaining system reserve value is the lowest. Therefore, the MES configuration method considering the system reserve value also has a certain cost advantage in the system operation when the system supply is insufficient.

VI. Conclusion

In this paper, a MES optimization configuration model for an IES is established. We consider the system operation mode and system reserve value under the environment of a reserve market. For system uncertainty caused by renewable energy access, the model can solve the problem of insufficient system reserve, which is conducive to giving full play to the flexibility and reserve value of the system. The following conclusions are drawn from our study.

1) The MES configuration of the system reserve value is conducive to improving the income of an IES including renewable energy in the reserve market and reducing the annual investment cost of electricity, gas and heat storage.

2) Different reserve service prices significantly affect the annual investment cost of the configuration. With the increase in price of the medium and long-term reserve service, the annual investment cost gradually and slowly decreases. Affected by the energy storage life and market constraints, the annual investment cost will rebound and increase after reaching the limit.

3) Compared with the independent configuration the energy station's power storage, gas storage and heat storage, a combined configuration of electricity, gas and heat storage based on energy stations is conducive to reducing operating costs. More coupling corresponds to a lower investment cost.

4) When the system supply capacity is sufficient or insufficient, the MES configuration considering the system reserve value is beneficial for improving system reserve value and reducing system operating cost.

VII. Outlook

In the future, in terms of the form of participation of the reserve market, further consideration should be given to the combination of medium- and long-term reserve service contracts and short-term reserve services. Based on the contract price of medium- and long- term reserve service and the price of short-term reserve service, the participation amount of medium- and long-term reserve service is allocated to give full play to the benefits of participating in the reserve market.

References

[1] C. R. Upshaw, J. D. Rhodes, and M. E. Webber, "Modeling electric load and water consumption impacts from an integrated thermal energy and rainwater storage system for residential buildings in Texas," *Applied Energy*, vol. 186, pp. 492–508, Jan. 2017.

[2] X. X. Zhou, Q. Zhao, Y. Q. Zhang, and L. Sun, "Integrated energy production unit: An innovative concept and design for energy transition toward low-carbon development," *CSEE journal of power and energy systems*, vol. 7, no. 6, pp. 1133–1139, Nov. 2021.

[3] W. L. Wang, D. Wang, H. J. Jia, Z. Y. Chen, B. Q. Guo, H. M. Zhou, and M. H. Fan, "Review of steady-state analysis of typical regional integrated energy system under the background of energy internet," *Proceedings of the CSEE*, vol. 36, no. 12, pp. 3292–3305, Jun. 2016.

[4] M. X. Liu, Y. Shi, and F. Fang, "A new operation strategy for CCHP systems with hybrid chillers," *Applied Energy*, vol. 95, pp. 164–173, Jul. 2012.

[5] Y. Li and Y. H. Han, "A module-integrated distributed battery energy storage and management system," *IEEE Transactions on Power Electronics*, vol. 31, no. 12, pp. 8260–8270, Dec. 2016.

[6] K. M. Muttaqi, M. R. Islam, and D. Sutanto, "Future power distribution grids: Integration of renewable energy, energy storage, electric vehicles, superconductor, and magnetic bus," *IEEE Transactions on Applied Superconductivity*, vol. 29, no. 2, pp. 3800305, Mar. 2019.

[7] X. P. Zhang, M. Shahidehpour, A. Alabdulwahab, and A. Abusorrah, "Optimal expansion planning of Energy hub with multiple energy infrastructures," *IEEE Transactions on Smart Grid*, vol. 6, no. 5, pp. 2302–2311, Sep. 2015.

[8] M. Salimi, H. Ghasemi, M. Adelpour, and S. Vaez-Zadeh, "Optimal planning of energy hubs in interconnected energy systems: a case study for natural gas and electricity," *IET Generation, Transmission & Distribution*, vol. 9, no. 8, pp. 695–707, May 2015.

[9] L. Z. Jiang, Z. H. Bie, T. Long, H. P. Xie, and Y. Xiao, "Distributed energy management of integrated electricity-thermal systems for high-speed railway traction grids and stations,". *CSEE journal of power and energy systems*, vol. 7, no. 3, pp. 541–554, May 2021.

[10] A. Dolatabadi, B. Mohammadi-Ivatloo, M. Abapour, and S. Tohidi, "Optimal stochastic design of wind integrated energy hub," *IEEE Transactions on Industrial Informatics*, vol. 13, no. 5, pp. 2379–2388, Oct. 2017.

[11] M. Momayyezan, D. B. W. Abeywardana, B. Hredzak, and V. G. Agelidis, "Integrated reconfigurable configuration for battery/ultracapacitor hybrid energy storage systems," *IEEE Transactions on Energy Conversion*, vol. 31, no. 4, pp. 1583–1590, Dec. 2016.

[12] D. Zhu, S. Y. Yue, N. Chang, and M. Pedram, "Toward a profitable grid-connected hybrid electrical energy storage system for residential use," *IEEE Transactions on Computer-Aided Design of Integrated Circuits and Systems*, vol. 35, no. 7, pp. 1151–1164, Jul. 2016.

[13] P. J. Mago and L. M. Chamra, "Analysis and optimization of CCHP systems based on energy, economical, and environmental considerations," *Energy and Buildings*, vol. 41, no. 10, pp. 1099–1106, Oct. 2009.

[14] Y. H. Yang, W. Pei, and Z. P. Qi, "Planning method for hybrid energy microgrid based on dynamic operation strategy," *Automation of Electric Power Systems*, vol. 36, no. 19, pp. 30–36, 52, Oct. 2012.

[15] L. Guo, W. J. Liu, J. J. Cai, B. W. Hong, and C. S. Wang, "A two-stage optimal planning and design method for combined cooling, heat and power microgrid system," *Energy Conversion and Management*, vol. 74, pp. 433–445, Oct. 2013.

[16] B. Zeng, J. H. Zhang, X. Yang, J. H. Wang, J. Dong, and Y. Y. Zhang, "Integrated planning for transition to low-carbon distribution system with renewable energy generation and demand response," *IEEE Transactions on Power Systems*, vol. 29, no. 3, pp. 1153–1165, May 2014.

[17] Q. Chen, J. H. Hao, L. Chen, Y. H. Dai, F. Xu, and Y. Min, "Integral transport model for energy of electric-thermal integrated energy system," *Automation of Electric Power Systems*, vol. 41, no. 13, pp. 7–13, 69, Jul. 2017.

[18] C. Wu, W. Tang, M. K. Bai, L. Zhang, and Y. X. Cai, "Energy router based planning of energy internet at user side," *Automation of Electric Power Systems*, vol. 41, no. 4, pp. 20–28, Feb. 2017.

[19] F. Barati, H. Seifi, M. S. Sepasian, A. Nateghi, M. Shafie-Khah, and J. P. S. Catalão, "Multi-period integrated framework of generation, transmission, and natural gas grid expansion planning for large-scale systems," *IEEE Transactions on Power Systems*, vol. 30, no. 5, pp. 2527–2537, Sep. 2015.

[20] F. Zhao, C. H. Zhang, B. Sun, and D. J. Wei, "Three-stage collaborative global optimization design method of combined cooling heating and power," *Proceedings of the CSEE*, vol. 35, no. 15, pp. 3785–3793, Aug. 2015.

[21] J. Wang, W. Gu, S. Lu, C. L. Zhang, Z. H. Wang, and Y. Y. Tang, "Coordinated planning of multi-district integrated energy system combining heating network model," *Automation of Electric Power Systems*, vol. 40, no. 15, pp. 17–24, Aug. 2016.

[22] J. Qiu, Z. Y. Dong, J. H. Zhao, Y. Xu, Y. Zheng, C. X. Li, and K. P. Wong, "Multi-stage flexible expansion co-planning under uncertainties in a combined electricity and gas market," *IEEE Transactions on Power Systems*, vol. 30, no. 4, pp. 2119–2129, Jul. 2015.

[23] Z. H. Bie, X. Wang, and Y. Hu, "Review and prospect of planning of energy internet," *Proceedings of the CSEE*, vol. 37, no. 22, pp. 6445–6462, Nov. 2017.

[24] M. Sechilariu, B. C. Wang, and F. Locment, "Building integrated photovoltaic system with energy storage and smart grid communication," *IEEE Transactions on Industrial Electronics*, vol. 60, no. 4, pp. 1607–1618, Apr. 2013.

[25] W. Xiong, Y. Q. Liu, W. H. Su, R. Hao, Y. Wang, and Q. Ai, "Optimal configuration of multi-energy storage in regional integrated energy system considering multi-energy complementation," *Electric Power Automation Equipment*, vol. 39, no. 1, pp. 118–126, Jan. 2019.

[26] M. Geidl, G. Koeppel, P. Favre-Perrod, B. Klockl, G. Andersson, and K. Frohlich, "Energy hubs for the future," *IEEE Power and Energy Magazine*, vol. 5, no. 1, pp. 24–30, Jan./Nov. 2007.

[27] M. Geidl and G. Andersson, "A modeling and optimization approach for multiple energy carrier power flow," in *Proceedings of 2005 IEEE Russia Power Tech*, 2005, pp. 1–7.

[28] J. Z. Zhu, Q. Z. Ye, J. Zou, P. P. Xie, and P. Z. Xuan, "Short-term operation service mechanism of ancillary service in the UK electricity market and its enlightenment," *Automation of Electric Power Systems*, vol. 42, no. 17, pp. 1–8, 86, Sep. 2018.

[29] Z. N. Wei, S. D. Zhang, G. Q. Sun, H. X. Zang, S. Chen, and S. Chen, "Power-to-gas considered peak load shifting research for integrated electricity and natural-gas energy systems," *Proceedings of the CSEE*, vol. 37, no. 16, pp. 4601–4609, Aug. 2017.

[30] C. M. Carlos and P. Sánchez-Martín, "Integrated power and natural gas model for energy adequacy in short-term operation," *IEEE Transactions on Power Systems*, vol. 30, no. 6, pp. 3347–3355, Nov. 2015.

[31] Z. G. Li, W. C. Wu, M. Shahidehpour, J. H. Wang, and B. M. Zhang, "Combined heat and power dispatch considering pipeline energy storage of district heating network," *IEEE Transactions on Sustainable Energy*, vol. 7, no. 1, pp. 12–22, Jan. 2016.

[32] X. D. Yang, Y. B. Zhang, J. J. Lu, B. Zhao, F. T. Huang, J. Qi, and H. W. Pan, "Blockchain-based automated demand response method for energy storage system in an energy local network," *Proceedings of the CSEE*, vol. 37, no. 13, pp. 3703–3716, Jul. 2017.

[33] B. Lunz, H. Walz, and D. U. Sauer, "Optimizing vehicle-to-grid charging strategies using genetic algorithms under the consideration of battery ag-

ing," in *Proceedings of IEEE Vehicle Power and Propulsion Conference*, Chicago, 2011, pp. 1–7.
[34] M. Abeysekera, J. Wu, N. Jenkins, and M. Rees, "Steady state analysis of gas networks with distributed injection of alternative gas," *Applied Energy*, vol. 164, pp. 991–1002, Feb. 2016.
[35] S. Pazouki and M. R. Haghifam, "Optimal planning and scheduling of energy hub in presence of wind, storage and demand response under uncertainty," *International Journal of Electrical Power & Energy Systems*, vol. 80, pp. 219–239, Sep. 2016.
[36] W. L. Wang, D. Wang, H. J. Jia, Z. Y. Chen, B. Q. Guo, H. M. Zhou, and M. H. Fan, "Steady state analysis of electricity-gas regional integrated energy system with consideration of NGS network status," *Proceedings of the CSEE*, vol. 37, no. 5, pp. 1293–1304, Mar. 2017.
[37] DIW Berlin. (2019, May 17) DIETER. [Online]. Available: https://www.diw.de/de/diw_01.c.508843.de/forschung_beratung/nachhaltigkeit/umwelt/verkehr/energie/modelle/dieter/dieter.html.

Xun Dou received B.S., M.S. and Ph.D. degrees from Southeast University, China in 2001, 2004 and 2012, respectively. She is a Professor at Nanjing Tech University. From 2015 to 2016, she was a visiting scholar at the School of Mechanical Engineering, UCLA. She is the author of more than 20 articles, and has introduced more than 10 inventions. Her research interests include integrated energy systems, power markets and power economics, demand response, and power planning.

Jun Wang received B.S. and M.S. degrees in Electrical Engineering and Automation from Nanjing Tech University, China, in 2017 and 2020, respectively. He is currently an Engineer with the Research Institute of NARI Technology Co., Ltd., Nanjing, China. His research interests include integrated energy systems, power markets and power economics.

Zhenyuan Zhang received a B.S. degree from Chang'an University, Xi'an, China, and a Ph.D. degree from the University of Texas at Arlington, Arlington, USA, in 2007 and 2015, respectively. He is currently a Professor of the School of Energy Science and Engineering in University of Electronic Science and Technology of China (UESTC). His research interests include power system analysis and power system optimization. He has also been involved in smart grids, renewable energy, electrical safety analysis, arc flash analysis and power market researches. Since 2010, he has served as the project associate for the IEEE/NFPA Arc Flash Research Project.

Min Gao received a Ph.D. degree in Electrical Engineering and an M.S. degree in Electrical Engineering from the University of California, Los Angeles, USA, and a B.E. degree in Electrical Engineering and Automation from Nanjing Tech University, China. He was a visiting scholar with Max Planck Institute for Software Systems, Germany, and State Key Laboratory of VLSI and Systems, Fudan University, China. His research interests include energy internet, machine learning, formal verification, EDA, cloud computing, IoT, and heterogeneous computing.